International Journal of Electrical, Electronic and Communication Sciences
ISSN: 2517-9438
Vol:10, No:5, 2016

The Stability Analysis and New Torque Control Strategy of Direct-Driven PMSG Wind Turbines

Jun Liu, Feihang Zhou, Gungyi Wang

***Abstract*—**This paper expounds on the direct-driven PMSG wind power system control strategy, and analyses the stability conditions of the system. The direct-driven PMSG wind power system may generate the intense mechanical vibration, when wind speed changes dramatically. This paper proposes a new type of torque control strategy, which increases the system damping effectively, mitigates mechanical vibration of the system, and enhances the stability conditions of the system. The simulation results verify the reliability of the new torque control strategy.

***Keywords*—**Damping, direct-driven PMSG wind power system, mechanical vibration, torque control.

I. Introduction

WITH the global climate problem increasingly prominent and non-renewable energy being consumed largely, the utilization and development of renewable energy begin to get high attention. As the fastest growing renewable energy sources in the recent years [1], wind power utility and research have much practical value. Because there is no the gearbox and the excitation control system in the direct-driven PMSG power system (PMSWG), it has a higher reliability, and its efficiency is higher than other generators, it gradually becomes the mainstream of wind power system model [2].

At present, domestic and foreign policy for the control of wind turbines had a very in-depth study. So, there are some new control methods, such as: gain scheduling control [3], sliding mode control [4] and intelligent control method [5], and effective to solute the problems that occurs at maximum wind power point tracking control. In actual control, PI control is still the most widely used. However, the method of tuning PI parameters is still based on the domain experience and trial-and-error method. This paper, by using feed-forward decoupling control and PI parameter tuning to inner current loop, effectively deduces the state space model of whole control system, and then analyzes the state-space model to meets the stability conditions of the control system, and tunes the control parameters at last.

For the traditional torque control method under PI control, it is unable to mitigate severe mechanical vibration of wind power system caused by dramatic changes of wind speed, this paper proposes a new type of torque control strategy, which can enhance system damping and mitigate mechanical vibration of the system. The simulation results verify the superiority and feasibility of the new torque control strategy.

Liu Jun, Zhou Feihang and Wang Gungyi are with School of Automation and Information Engineering, Xi'an University of Technology, (e-mail: liujun0310@sina.com, qq987102679@126.com, x5675602@gmail.com).

II. Wind Power Mathematical Model

PMSWG is mainly made of wind machine, direct drive shaft, the permanent magnet synchronous generator, generator-side converter and the grid-side inverter. Its structure is shown in Fig. 1.

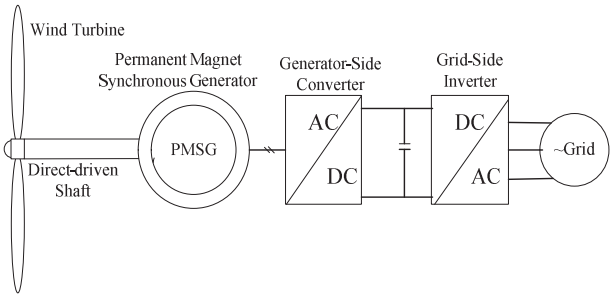

Fig. 1 The structure diagram of Permanent magnet synchronous wind power system

A. Winding Machine Model

According to the theory of Bates, the mechanical power of winding machine is given by:

$$P_{\text{tur}} = \frac{1}{2}\pi\rho R^2 C_P(\beta,\lambda)v^3 \tag{1}$$

$$\lambda = \frac{R\omega}{v} \tag{2}$$

The formula of Wind power conversion coefficient is as:

$$C_P(\beta,\lambda) = 0.58(116\lambda_{\text{m}} - 0.4\beta - 5)e^{-21\lambda_{\text{m}}} \tag{3}$$

with

$$\lambda_{\text{m}} = \frac{1}{\lambda + 0.08\beta} - \frac{0.035}{\beta^3 + 1} \tag{4}$$

The output power of Winding machine is as:

$$T_{\text{tur}} = \frac{P_{\text{tur}}}{\omega} = \frac{1}{2}\pi\rho R^3 C_P(\beta,\lambda)v^2/\lambda \tag{5}$$

where ρ is the air density (kg/m^3), R is the radius of the blade [m], v is the wind speed (m/s).

B. Model of PSWG

In the synchronous reference frame (d-q), the current

equations for PMSM are expressed as follows [6]-[8]:

$$\begin{cases} \dfrac{\mathrm{d}i_d}{\mathrm{d}t} = -\dfrac{R_s}{L} i_d + n_p \omega i_q + \dfrac{1}{L} u_d \\ \dfrac{\mathrm{d}i_q}{\mathrm{d}t} = -\dfrac{R_s}{L} i_q - n_p \omega i_d - \dfrac{n_p \omega \phi}{L} + \dfrac{1}{L} u_q \end{cases} \tag{6}$$

Electromagnetic torque is given by

$$T_{\text{gen}} = \frac{3}{2} n_p \phi i_q \tag{7}$$

and the corresponding electromagnetic power is as:

$$P_{\text{gen}}=T_{\text{gen}}\omega \tag{8}$$

where L is state reluctance, R_s is state resistance, ϕ is the permanent flux, n_p is pole pairs, i_d and i_q re d-axis and q-axis currents respectively, u_d and u_q are d-axis and q-axis voltages respectively.

C. Current Feed-Forward Decoupling

Equation (6) exists coupling terms $n_p\omega L i_q$ and $-n_p\omega(i_d+\phi/L)$, let

$$\begin{cases} v_d = n_p \omega L i_q + u_d \\ v_q = -n_p \omega (L i_d + \phi) + u_q \end{cases} \tag{9}$$

Ignoring the converter model, consider

$$\begin{cases} u_d^* = u_d = v_d - n_p \omega L i_q \\ u_q^* = u_q = v_q + n_p \omega (L i_d + \phi) \end{cases} \tag{10}$$

So, PMSM model can be expressed as

$$\begin{cases} \dfrac{\mathrm{d}i_d}{\mathrm{d}t} = -\dfrac{R_s}{L} i_d + \dfrac{1}{L} v_d \\ \dfrac{\mathrm{d}i_q}{\mathrm{d}t} = -\dfrac{R_s}{L} i_q + \dfrac{1}{L} v_q \end{cases} \tag{11}$$

written in the form of transfer function, that is,

$$G_i(s) = \frac{i_d(s)}{v_d(s)} = \frac{i_q(s)}{v_q(s)} = \frac{1}{Ls + R_s} \tag{12}$$

where, $i_d(s)$ and $v_d(s)$ are the instruction signals of SVPWM.

D. Current Loop PI Control

According to (12), we can see that, *dq*-coordinates current control can use the same PI controller parameter (k_{p1}, k_{i1}). Its control diagram is show in Fig. 2.

The *dq*-coordinates current control open loop transfer function:

$$G(s) = (k_{p1} + \frac{k_{i1}}{s}) \frac{1}{Ls + R_s} = \frac{k_{p1}s + k_{i1}}{s(Ls + R_s)} \tag{13}$$

For i_d / i_d^* and i_q / i_q^*, we can have

$$\varphi(s) = \frac{i_d}{i_d^*} = \frac{i_q}{i_q^*} = \frac{k_{p1}s + k_{i1}}{Ls^2 + (R_s + k_{p1})s + k_{i1}} \tag{14}$$

PI parameters using a first-order tuning, (13) and (14) can be rewritten as

$$G(s) = \frac{k_{i1}(\frac{k_{p1}}{k_{i1}} s + 1)}{R_s s(\frac{L}{R} s + 1)} = \frac{k_{i1}}{R_s s} = \frac{1}{Ts} \tag{15}$$

$$\varphi(s) = \frac{k_{i1}}{R_s s + k_{i1}} = \frac{1}{Ts + 1} \tag{16}$$

where $k_{p1}=k_{i1}*L/R_s$, $T=R_s/k_{i1}$. From (16), the current circle can be seen as a one order inertial.

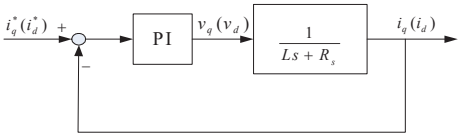

Fig. 2 The current inner control block diagram

E. Mechanical Transmission Shaft Model

In the PMSWG, the flexibility of shaft is much low, so the rigid body model [9] is used here. Ignoring the friction damping, we can see that:

$$J\frac{\mathrm{d}\omega}{\mathrm{d}t}=T_{tur}-T_{gen} \tag{17}$$

where, J is the inertia of PSWG.

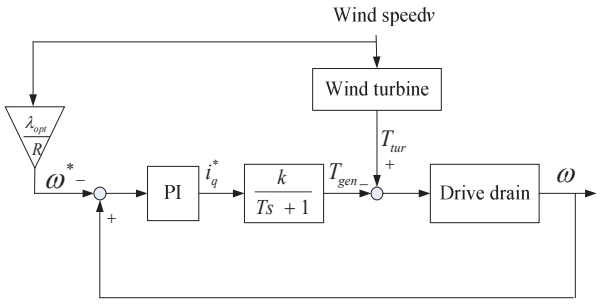

Fig. 3 The block diagram of speed feedback control

F. Speed Loop PI Control

The block diagram of speed loop control is shown in Fig. 3, and the responding parameters of PI controller can be defined as k_p and k_i, k=1.5$n_p\phi$.

Define $e = \omega - \omega^*$, the transfer function from e to electromagnetic power T_{gen} can be expressed as:

$$G_0(s)=\frac{T_{gen}(s)}{e\ (s)}=\frac{kk_i(k_ps/k_i+1)}{s(Ts+1)} \tag{18}$$

III. Wind Power System Stability Analysis

A. State Model

Take $x_1=\omega$, $dx_2/dt=e$, $x_3=T_{gen}$, from (17), we can get that

$$\frac{dx_1}{dt}=-\frac{1}{J}x_3+\frac{1}{J}T_{tur} \tag{19}$$

$$\frac{dx_2}{dt}=x_1-\omega^* \tag{20}$$

From Fig. 3, we can get that

$$i_q^*=k_p\frac{dx_2}{dt}+k_ix_2=\frac{T}{k}\frac{dx_3}{dt}+\frac{1}{k}x_3 \tag{21}$$

From (19)-(21), it is calculated that

$$\frac{dx_3}{dt}=\frac{kk_p}{T}x_1+\frac{kk_i}{T}x_2-\frac{1}{T}x_3-\frac{kk_p}{T}\omega^* \tag{22}$$

So,

$$\dot{x}=Ax+Bu \tag{23}$$

where

$$A=\begin{bmatrix}0 & 0 & -\frac{1}{J}\\ 1 & 0 & 0\\ \frac{kk_p}{T} & \frac{kk_i}{T} & -\frac{1}{T}\end{bmatrix},\quad B=\begin{bmatrix}\frac{1}{J} & 0\\ 0 & -1\\ 0 & -\frac{kk_p}{T}\end{bmatrix},\quad u=[T_{tur}\quad \omega^*]^{\mathrm{T}}.$$

B. Stability Analysis

The system characteristic equation:

$$d(s)=|Is-A|=s^3+\frac{1}{T}s^2+\frac{kk_p}{JT}s+\frac{kk_i}{JT}=0 \tag{24}$$

The Routh criterion:

s^3	1	$\frac{kk_p}{JT}$
s^2	$\frac{1}{T}$	$\frac{kk_i}{JT}$
s^1	$\frac{k(k_p/T-k_i)}{J}$	
s^0	$\frac{kk_i}{JT}$	

The stability condition of the system is, $1/T>0$, $k(k_p/T-k_i)/J>0$, $kk_i/JT>0$, namely, $T>0$, $k_p>0$, $k_i>0$, $k_i/k_p<1/T$.

C. PI Parameter Tuning of Outer Loop Rotor Speed

After PI correction the magnitude frequency curves of $G_0(s)$ are shown in three cases as shown in Fig. 4.

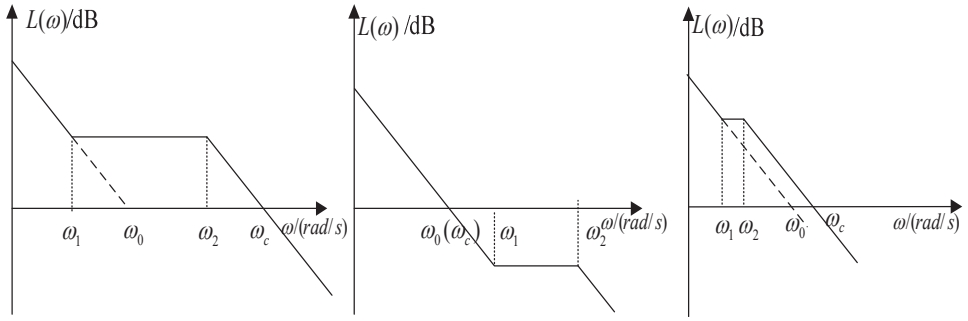

(a) (b) (c)

Fig. 4 The amplitude-versus-frequency curves of $G_0(s)$

In Fig. 4, $\omega_0=kk_i$, $\omega_1=k_i/k_p$, $\omega_2=1/T$, ω_c are the crossover frequency of $G_0(s)$. Compared with Figs. 4 (a) and (c), we can see that Fig. 4 (b) has the wider medium bandwidth. That means that there is better stability margin, higher response speed, and better dynamic performance in Fig. 4 (b). In Figs. 4 (a)-(c), the slope at high frequency is -20*dB/dec,* that shows that they have the same high ability of noise-resistant. The factors that determine the low frequency characteristics are the type of system and the static gain kk_i. Figs. 4 (a)-(c) are Type I system; however, their static gain value will be different.

According to Fig. 4 (a):

$$\omega_1=\frac{k_i}{k_p}<\omega_0=kk_i<\omega_2=\frac{1}{T}$$

According to Fig. 4 (b):

$$\omega_0=kk_i<\omega_1=\frac{k_i}{k_p}<\omega_2=\frac{1}{T}$$

According to Fig. 4 (c):

$$\omega_1=\frac{k_i}{k_p}<\omega_2=\frac{1}{T}<\omega_0=kk_i$$

when T does not vary with the static gain. Amplitude-versus-frequency curve of Fig. 4 (c) is the best, and the low frequency characteristic is the best. According to the theory of the three frequency band, the amplitude-versus-frequency curves of $G_0(s)$ should like the curve in Fig. 4 (c).

In Fig. 4 (c), if $\omega_2^2 = \omega_0\omega_1$, then $kk_i^2T^2 = k_p$, $k_p > k > Tk_i$.

IV. New Torque Control Strategy

A. Mechanical Vibration Analysis of Wind Power System

The object of PMSG wind power generation system is to capture the maximum wind energy, when the wind speed is lower than the rated wind speed. The control strategy is using outer loop rotor speed control, with the wind turbine running at optimal tip speed ratio to realize the maximum wind power tracking control. As the wind speed is time varying, there is uncertainty, stochasticity and intermittent in the control. The traditional torque control strategy with the single control target of maximum wind energy will cause the wind turbine mechanical torque T_{tur} fluctuation, resulting in rotor speed fluctuations. Rotor speed fluctuation will influence tip speed ratio λ and wind power coefficient C_P, and increase volatility of T_{tur}, makes the system have strong mechanical vibration. Thus it can be seen that the suppression of the rotor speed fluctuation of the wind power system is beneficial to mitigating of the mechanical vibration of the system.

From (17), the rotor speed dynamic can be expressed as:

$$G_{\Delta}(s) = \frac{\Delta\omega(s)}{\Delta T_{tur}(s) - \Delta T_{gen}(s)} = \frac{1}{Js} \tag{25}$$

From (20), the output torque fluctuation of the wind turbine and the electromagnetic torque ripple of the generator will inevitably lead to the fluctuation of the rotor speed. At the steady state, if $\Delta T_{gen} = \Delta T_{tur}$, $\Delta\omega$ is equal to 0, that is to say, the mechanical torque of the wind turbine must be tracked in real time by the electromagnetic torque. That not only needs that T to approach zero, and the mechanical torque of the wind turbine should be measured or estimated on line, which will undoubtedly increase the cost of wind power system. Based on this, this paper proposes a new type of torque control strategy to mitigate the mechanical fluctuation of the system.

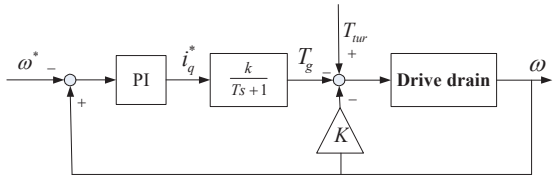

(a)

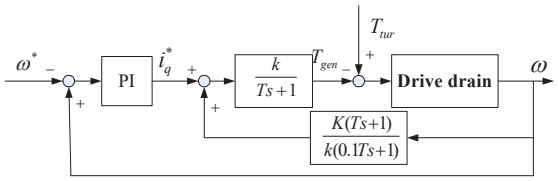

(b)

Fig. 5 New torque control block diagram

B. New Torque Control Strategy

The electromagnetic torque is disassembled into two parts, one part is the electromagnetic torque of the rotor speed outer loop control, T_g; the other is related to the speed, $K\omega$. The control diagram of the system is shown in Fig. 5, because the system uses the inner current loop control, only the corresponding compensation introduced into current control can the control requirements be met. Fig. 5 (a) can be expressed to Fig. 5 (b). So, there is:

$$T_{gen} = T_g + K\omega \tag{26}$$

The rotor speed dynamic can be expressed as

$$G_{\Delta 0}(s) = \frac{\Delta\omega(s)}{\Delta T_{tur}(s) - \Delta T_g(s)} = \frac{1}{Js + K} \tag{27}$$

The $G_{\Delta 0}$(s) as a first order inertial element, has some filtering effect. The increase of K can reduce the static gain of $1/K$ of the $G_{\Delta 0}$(s). It can reduce the influence of the fluctuation of the mechanical torque and electromagnetic torque on the rotor speed fluctuation. While larger K can reduce the mechanical vibration of the system, it has also a negative effect on the dynamic performance of the system. Therefore, the variable gain control method is introduced. For a long time, control engineering community has an experimental understanding:" big error, small gain; small error, large gain". Variable gain PID control, fuzzy control, intelligent control, is based on this [1]. In this paper, the fuzzy method is used to deal with K, as shown in Fig. 6. Specific steps are as:

Step 1. Quantize the variables e and K;
Step 2. Determine the proper memberships function of e and K;
Step 3. Form the fuzzy rule table;
Step 4. According to fuzzy rule, reason and calculate K value.

The variation range of the deviation e is $[-e_{max}, e_{max}]$, $e_{max}=\lambda_{opt}*v_{max}/R$; The change range of K is $[0,K_{max}]$, K_{max} is the maximum value, it generally take large value, in this paper, K_{max}=1e+6; The scaling factor $K_e=n/e_{max}$, $K_m=K_{max}/m$, $n=m$=6; The fuzzy domain of e is {-6, -5, -4, -3, -2, -1, 0, 1, 2, 3, 4, 5, 6}, the fuzzy domain of k is {0, 1, 2, 3, 4, 5, 6}; The fuzzy rules is shown in Table I.

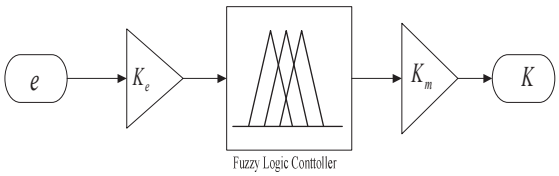

Fig. 6 Fuzzy logic diagram

TABLE I
The Fuzzy Rule

e	NB	NM	NS	ZE	PS	PM	PB
K	ZE	PS	PM	PB	PM	PS	ZE

C. The Influence of the New Type Torque Control on System Stability

From assumption of $z_1 = x_1$, $z_2 = x_2$, and $z_3 = T_g$, we can have:

$$\dot{z} = A_1 z + B_1 v \tag{28}$$

where,

$$A_1 = \begin{bmatrix} -\frac{K}{J} & 0 & -\frac{1}{J} \\ 1 & 0 & 0 \\ \frac{kk_p}{T} & \frac{kk_i}{T} & -\frac{1}{T} \end{bmatrix}, \quad B_1 = \begin{bmatrix} \frac{1}{J} & 0 \\ 0 & -1 \\ 0 & -\frac{kk_p}{T} \end{bmatrix}$$

$$v = [T_{tur} \quad \omega^*]^{\mathrm{T}}$$

Now, the characteristic equation of system:

$$d_0(s) = |Is - A_1| = s^3 + (\frac{K}{J} + \frac{1}{T})s^2 + \frac{kk_p + K}{JT}s + \frac{kk_i}{JT} = 0 \tag{29}$$

The Routh-Hurwitz criterion:

$$\begin{array}{lll} s^3 & 1 & \frac{kk_p + K}{JT} \\ s^2 & \frac{K}{J} + \frac{1}{T} & \frac{kk_i}{JT} \\ s^1 & M & \\ s^0 & \frac{kk_i}{JT} & \end{array}$$

and the stability condition of the system is:

$$K/J+1/T>0;\ kk_i/JT>0;$$

$$M=[(K/J+1/T)(K+kk_p)-kk_i]/(KT+J)>0.$$

when $K>0$, $T>0$, $k_i>0$, $k_p>0$, the system must satisfy:

$$kk_i/JT>0,\ K/J+1/T>0.$$

when $M>0$, the system must be satisfied:

$$(K/J+1/T)(K+kk_p)-kk_i>0$$

Take consideration that $(K/J+1/T)(K+kk_p)-kk_i=0$, then:

$$\frac{K^2}{J} + (\frac{1}{T} + \frac{kk_p}{J})K + \frac{kk_p}{T} - kk_i = 0 \tag{30}$$

The Routh criterion:

$$\begin{array}{lll} K^2 & \frac{1}{J} & \frac{kk_p}{T} - kk_i \\ K^1 & \frac{1}{T} + \frac{kk_p}{J} & \\ K^0 & \frac{kk_p}{T} - kk_i & \end{array}$$

when $k_i / k_p < 1/T$, (30) exists negative real roots in (30), that is: when $K> 0$, $M> 0$, the system is stable. That is, if k_i, k_p, and T don't vary, the new torque control can ensure stability of the system, namely, and does not affect the stability of torque control system.

V. Example Analysis and Verification

Under the Matlab/Simulink, a direct-driven PMSG wind power system simulation platform in detail is built to validate the new control strategy proposed. Wind power system parameters are shown in Table II.

TABLE II
Wind Power System Parameters

parameter	value
Blade radius R/m	28
Air density ρ/(kg·m^3)	1.225
inertial J/(kg·m^2)	1e4
Generator nominal power P_{gen}/MW	2
Generator pole pairs n_p	102
State resistance R_s/Ω	0.11
State reluctance L/H	0.000835
Permanent magnet flux ϕ/W_b	1.25
Maximum wind power coefficient C_P	0.467
optimum blade speed ratio λ_{opt}	7.9540

By using the random variation of wind speed model to simulate the change of wind speed in the actual wind field, as shown in Fig. 7. The average wind speed is 12 m/s; the random fluctuation range of wind speed is at 11 m/s to 13 m/s.

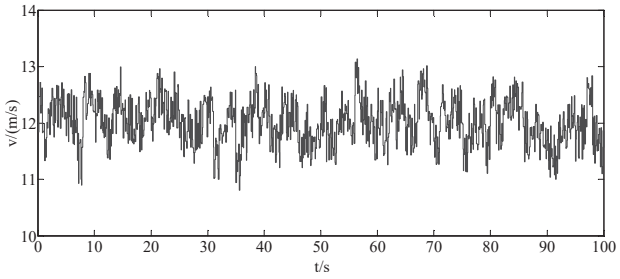

Fig. 7 Characteristics of wind

Take $k_p = 2k = 382.5$, T = 1e-3, so that $k_i = (k_p/(kT^2))0.5 = 20.5/T=1414$. Under the identical control parameters, rotor speed, wind energy utilization coefficient, tip speed ratio and power curve of traditional torque control strategy and the new torque control strategy of direct-driven PMSG wind power system as shown in Fig. 8-11. The characteristic root of the matrix A, the damping coefficient and the natural oscillation frequency of the group of control parameters are shown in Table III. When the $K=K_{max}$ is taken, the eigenvalues of the matrix A_1, the damping coefficient ξ and the natural oscillation frequency ω_n are shown in Table IV.

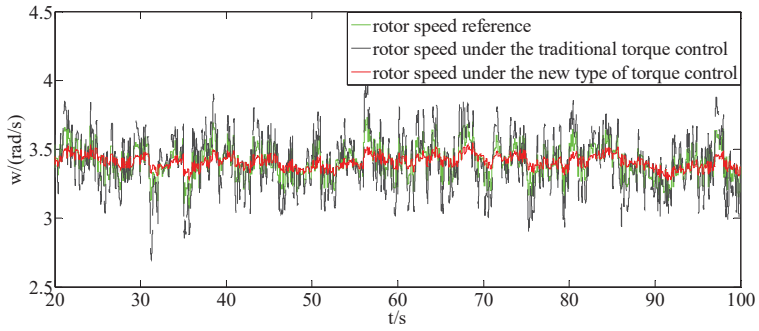

Fig. 8 Characteristics of rotor speed

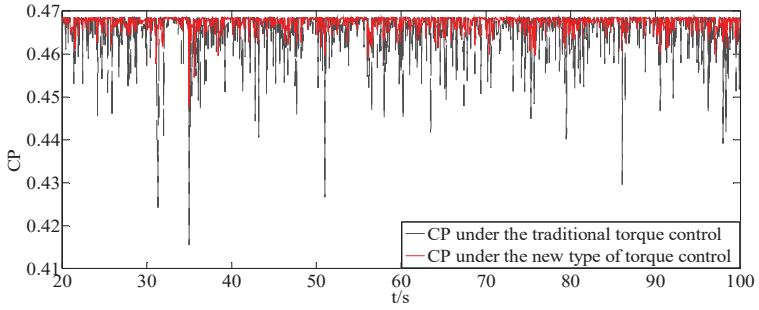

Fig. 9 Characteristics of C_P

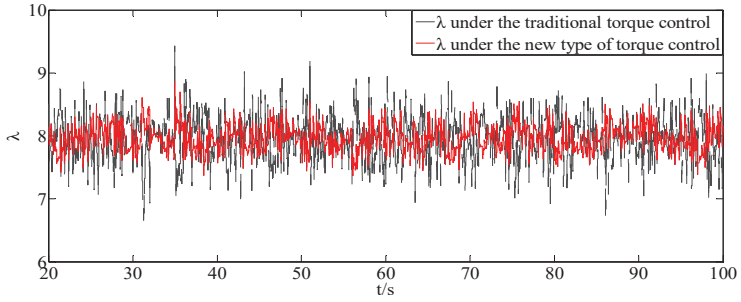

Fig.10 Characteristics of λ

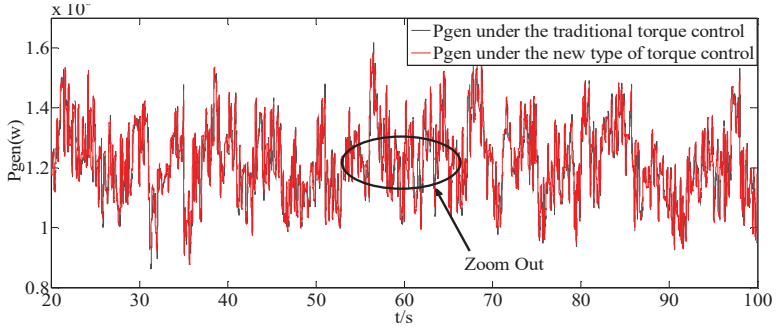

(a) Electromagnetic power

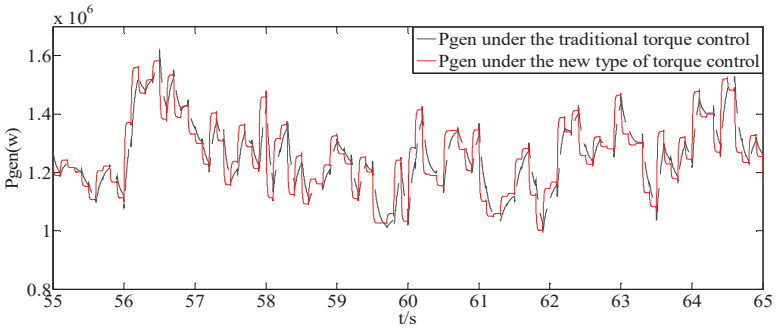

(b) Enlarged graph of ellipse region

Fig. 11 Characteristics of P_{gen}

From the simulation results, when the wind speed changes, compared with the traditional torque control strategy, the new torque control strategy obviously reduces the fluctuation of the rotor speed, wind energy utilization coefficient, tip speed ratio λ, mitigate the mechanical vibration of the system, and enhance the stability of the system. Fig. 11 shows that the electromagnetic power generated by the wind turbine generator scarcely changes much.

TABLE III
THE MATRIX A'S CHARACTERISTICS OF Λ, Ξ AND Ω_N

State variables	Characteristics roots λ_i	Damping coefficient ξ	Natural oscillation frequency ω_n
x_1	-992.66+0.00001i	close to 1	992.66
x_2	-3.67 + 3.71i	0.703	5.22
x_3	-3.67 - 3.71i	0.703	5.22

TABLE IV
THE MATRIX A_1'S CHARACTERISTICS OF Λ, Ξ AND Ω_N

State variables	Characteristics roots λ_i	Damping coefficient ξ	Natural oscillation frequency ω_n
z_1	-991.828	1	991.828
z_2	-107.9194	1	107.9194
z_3	-0.2526	1	0.2526

From the comparison of between Tables III and IV: when K is equal to K_{max} which is constant, the new torque control strategy is better than the traditional torque control strategy, the damping coefficient of each state variable of the system is increased. The natural frequency of the system determines the response speed of system, the dominant characteristic roots (poles) of the matrix A are $\lambda_{2,3}$=-3.67+3.71i, the corresponding natural frequency ω_n=5.22. The dominant characteristic root of matrix A_1 is λ_3=-0.2526, corresponding ω_n=0.2526, so the response speed of the system is reduced. That is to say, the system has a larger damping with the cost of losing some of the dynamic characteristics, and that further illustrates the necessity of variable gain.

VI. Conclusion

The traditional torque control strategy of direct-driven PSMG wind power system, with dramatic changes of wind speed, will cause wind turbine torque ripple and reference speed fluctuations calculated according to the optimal tip speed ratio method, result in the fluctuation of system rotor speed, wind energy utilization coefficient, tip speed ratio, make the system generate intense mechanical vibration. Based on above, this paper proposes a new type torque control strategy, and analyzes the influence of the new control strategy on the system. The simulation results indicate that the new type torque strategy can effectively increase the system damping, reduce the load and fatigue damage of the wind power system, and mitigate the mechanical vibration, which has important actual significance for the control of practical wind power system.

References

[1] Li S, Haskew T, Swatloski R P, et al. "Optimal and direct-current vector control of direct-driven PMSG wind turbines," *Power Electronics*, *IEEE Transactions on*, 2012, 27(5): 2325-2337.
[2] Yan J, Lin H, Feng Y, et al. "Improved sliding mode model reference adaptive system speed observer for fuzzy control of direct-drive permanent magnet synchronous generator wind power generation system," *IET Renewable Power Generation*, 2013, 7(1): 28-35.
[3] Bianchi F D, Mantz R J, Christiansen C F. "Gain scheduling control of variable-speed wind energy conversion systems using quasi-LPV models," *Control Engineering Practice*,2005,13(2):247-225.
[4] De Battista H, Mantz R J, Christiansen C F. "Dynamical sliding mode power control of wind driven induction generators," *IEEE Transactions on Energy Conversion*,2000,15(4):415-457.
[5] Simoes M G, Bose B K, Spiegel R J. "Fuzzy logic based intelligent control of a variable speed cage machine wind generation system," *IEEE Transaction on Power Electronics*,1997,12(1):87-95
[6] Shen Y, Li F, Wu D, et al. "dSpace based direct-driven permanent magnet synchronous wind power system modeling and simulation," *2012 UKACC International Conference on. IEEE*, 2012: 809-812.
[7] Trilla L, Bianchi F D, Gomis-Bellmunt O. "Linear parameter-varying control of permanent magnet synchronous generators for wind power systems," *IET Power Electronics 2014*, 7(3): 692-704.
[8] Kim K H, Jeung Y C, Lee D C, et al. "LVRT scheme of PMSG wind power systems based on feedback linearization," *Power Electronics, IEEE Transactions on*, 2012, 27(5): 2376-2384.
[9] Han Jingqing, "From PID to active disturbance rejection control," *IEEE Trans. Ind. Electro*,2008,56(3):900-906